The Production of High Carbon Steel Directly in Bloomery Process: Theoretical Bases and Metallographic Analyses of the Experiments Results

Adrian Wrona (PL)

The problem of steel[1] making in antiquity has intrigued researchers who specialize in ancient metallurgy for decades. In the course of research different explanations have prevailed in the scholarship. R. J. Forbes (1950, 405-412) in his classic work *Metallurgy in Antiquity* distinguished three main methods of steel production:

1. Steel obtained directly in the bloomery process. However, he points out that high carbon steel was only a small part of smelted bloom and was not able to fulfil the population's needs for a high-quality material used to produce the necessary tools. He argued his thesis by poor ores used by ancient smelters, low temperature of process, et cetera.
2. As a second method, Forbes mentions the possibility of decarburization of cast iron obtained during the smelting process, but he rejects the intentional receive of it in the reduction process. The fragments of pig iron occasionally found, mostly on the Roman metallurgical sites, are (according to Forbes) accidental by-products that have been abandoned as an useless and not suitable for further processing.
3. A third possibility is making steel by carburization of soft iron, commonly called *cementation* or *casehardening.*

This distinction came to form the basis our knowledge on the subject, and these methods became a basis for further studies and explanations about carburizing technique used in tool and weapon production. For a long time the third possibility was considered the main method for the preparation . It was justified by well known and well preserved blacksmithing techniques and confirmed in many written sources (Theophilus Presbyter 1998; Biringuccio 1540; Porta a Neopolitane 1638). Many ancient iron items also show signs of casehardening (Pleiner 2006, pp.200-202; Nosek 1966, pp.179-184; Piaskowski 1960, p.201, 220). However, it is worth noting here that it is the only method that is possible to identify in the final products, which were previously strongly processed. A blacksmith's treatment distorts the original structure of iron and makes impossible to identify the mechanism of primary carburization from reduction or post reduction stage. Some researchers argued for the possibility and legitimacy of steel obtained by decarburization of cast iron received in the bloomery process (Rehder 1989; Piaskowski 1958, pp.334-335). These arguments, however, did not become popular (Wagner 1990; Pleiner 2000, pp.247-250). The number of finds of fragments in the form of cast iron seems to indicate that they were unwanted and incidental products left in the debris. Decarburizing of cast iron is a much more difficult process than carburization and requires a more

[1] Chemically, the steel is a iron-carbon alloy (with other elements) with carbon content less than 2,11%. Pure iron does not occur in the nature. It can be received only in the laboratory. According to the technical literature it is assumed to designate this term to the product of bloomery process

advanced design than a typical blacksmith forge. A huge loss of material during the process in open forge suggests a low probability of using this method in antiquity. Despite the fact that the earliest cast iron finds in Europe come from the Roman period (Pleiner 2000, pp.247-250), the beginning of the intentional indirect iron-making process took place somewhere in 13th century (Knau, Beier and Sönnecken 2001; Lucas 2005, p.19) and the first information about decarburizing of pig iron in finery forge came from the turn of the 14th and 15th centuries (Radwan 1963, p.126).

Studies done in the past decade resulted in many new discoveries that gave a whole new perspective on the discussed topic. I will mention only the most important of them that inspired my paper. Experiment conducted by P. Crew and his team showed the tremendous easiness of obtaining cast iron in a bloomery furnace powered by hand operated bellows (Crew 2004). One of the conclusions contained in the papers devoted to the examinations of bloom produced in the experiment was a thesis that cast iron is an inevitable by-product of high carbon steel production rather than an occasional and isolated waste (Crew, et al. 2011, p.258). A team of Cracovian metallurgists made further progress. The high carburization observed by Z. Kędzierski and J. Stępiński (2006) on selected iron items and gromps with simultaneous occurrence of phosphorus eutectic prompted them to take a closer look at this relation. They observed that the presence of ferrite and iron phosphide makes possible the local appearance of the liquid phase at temperatures of about 1050˚C, which is easily achievable in the bloomery process. Because the diffusion rate of carbon in the liquid iron is incomparably higher than in the solid state, even brief appearance of the liquid phase allows its strong carburization. Then, during the smelt and further processing, the carbon diffuses into the surrounding ferritic parts, increasing the carburizing area and thereby alleviating the concentration gradients. The results of these studies indicate the possibility of obtaining a much larger amount of steel during the reduction process than allowed by the diffusion in solid state itself.

Another important step was taken by S. Williams and L. Sauder (Sauder 2010) who re-discovered the carburizing process in the so-called 'Aristotle furnace'. The same method of iron carburization is well known and used by Japanese swordsmiths and is called the jigane-oroshi process (Inoue 2002, p.196; Kapp, Kapp and Yoshihara 1987, pp.68-69). It was also known in modern Europe. The process described in Ole Evenstad's treatise on steel making technique (Evenstadt 1968, p.65) is based on the same mechanism as the two mentioned. Despite a number of editions of the treatise and numerous quotations in the specialist literature the process has not been thoroughly investigated before. This process consists of passing the low-carbon steel (iron) through the furnace heated to the right temperature. Iron falling down into the furnace heats up and, thanks to the carburizing atmosphere prevailing in the most parts of furnace, begins to absorb carbon. When it falls to the height of the tuyère, where the temperature reaches the melting point, the surface becomes partly melted. Then this partially melted portion drips to the hearth's bottom and creates partially carburized agglomerate.

The most recent studies (Wrona 2012) performed on the products of the process presented above revealed interesting mechanisms of this phenomenon. The structure observed on the cross-sections of ingots allows for the conclusion that this high degree of carburization was made possible by the partial melting of the batch. Metallographic observations of the samples' surfaces present a diversity of existing structures and reveal an uneven degree of carburization. The highest concentration of carbon observed on the cross-section (with content significantly exceeding 1.5%) was located in the

inner parts and arranged in layers with alternating bands of predominantly ferritic structure (see Figures 1, 5-6). The occurrence of such high carburized areas inside the ingots, combined with a very short (a few-minutes) duration of the process testify to local partial melting and strong carburizing of charge that falls to the bottom of the furnace creating a multi-layered clot. This thesis seems to be confirmed by the hypoeutectic structure observed in the cross-section of sample (see Figures 1-3) and the Widmanstätten ferrite educts (see Figures 4,6), which can be explained by local melting and overheating of steel. The coexistence in the adjacent space of hypereutectoid structures points to a further intensive diffusion of carbon to the surrounding areas (see Figures 1,3,7). The accurate characterization of changes in the boundaries of the two-phase coexistence region of the liquid and austenite in the presence of the high dynamics of transitions caused by changing carbon content and periodic temperature variations is not possible at the present time and requires further research and verifications. In addition to that highly carburized zone, there are also areas of the virtually unchanged, ferrite-pearlitic structure of the starting material (see Figure 5).

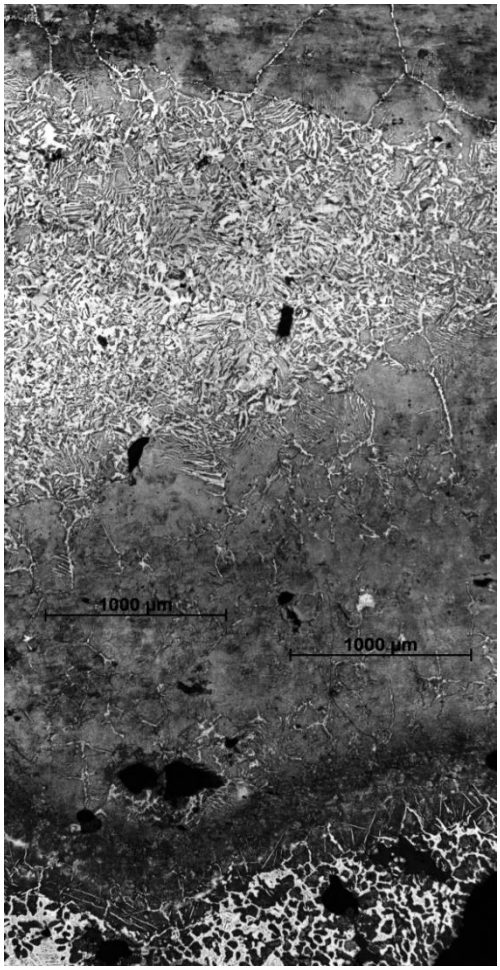

Fig 1. Micro-photograph of ingot Nr 2. Visible transition from hypoeutectic structure, by pearlite, to hypoeutectoid structure.

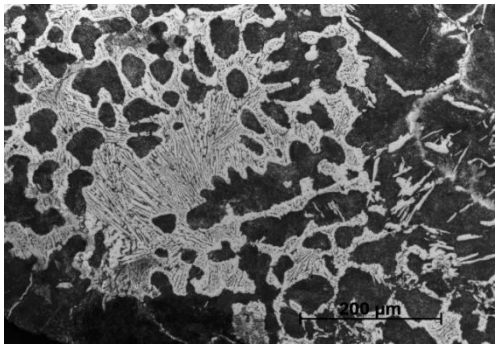

Fig 2. Micro-photograph of ingot Nr 2. Hypoeutectic structure, obtained by remelting and carburization in liquid state: pearlite and transformed ledeburite.

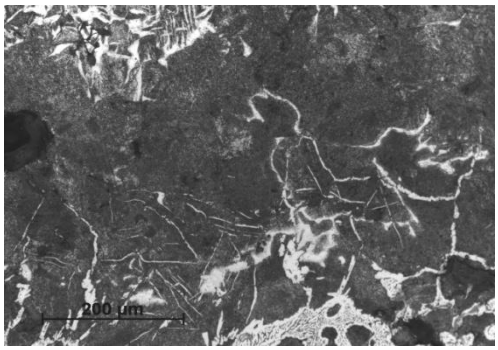

Fig 3. Micro-photograph of ingot Nr 2. Visible border between remelted part crystallized as an hypoeutectic alloy and structure shaped by diffusion processes: (from the bottom) ledeburite with pearlite, above pearlite with pro-eutectoid cementite, pearlite and pearlite with ferrite.

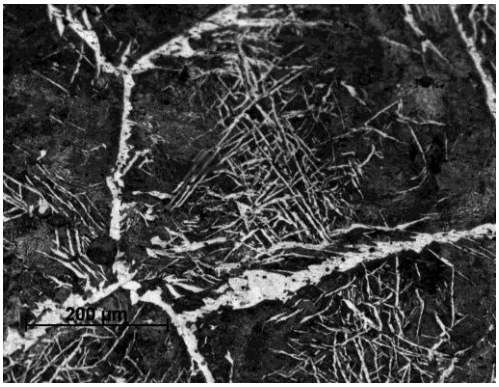

Fig 4. Micro-photograph of ingot Nr 2. Pearlite-ferritic structure. Ferritic grid at the grains boundaries and pearlitic area with Widmanstätten ferritie educts.

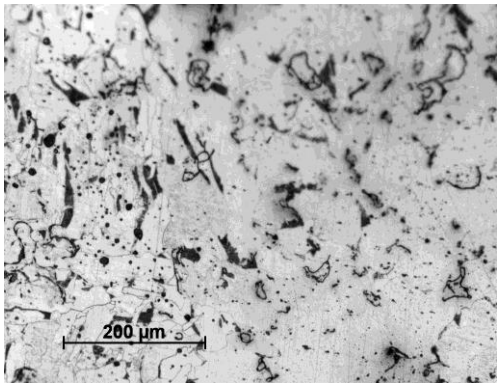

Fig 5. Micro-photograph of ingot Nr 2. Ferrite-pearlitic structure with numerous slag inclusions.

Fig 6. Micro-photograph of ingot Nr 2. Transition between pearlite-ferritic structure and more carburized pearlitic zone.

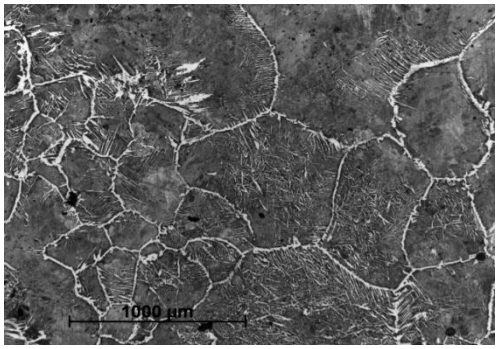

Fig 7. Micro-photograph of ingot Nr 2. Hypereutectoid structure – pearlite with pro-eutectoid cementite at the grains boundaries.

Recent experiments of the iron smelting shows that the same mechanism as in the carburizing in so-called 'Aristotle furnace' may occur in appropriate conditions, independently of phosphide eutectic, during the smelting operation. Iron with a high carbon content was obtained during four smelting operations performed in last year.

During one of the typical smelts in an ancient furnace, which took place in the workshops and training conducted by The Świętokrzyskie Association of Industrial Heritage in Kielce at The Culture and Archaeology Center in Nowa Słupia, an unusual result of the process was obtained. The bright silver colour of dispersed pieces of iron, which did not integrate with the proper bloom, looked strikingly similar to the pieces of Japanese tamahagane steel. While trying to forge one of these pieces the assumptions about the high carburization of sample were confirmed. Even during processing at high temperatures, it demonstrated a high hardness and low deformability. After forging the small bar and its hardening, it had a similar hardness like a file. It became clear that we had produced a high carbon steel pieces similar to the gromps, well known from Roman period production sites. Because of the shape of the iron pieces, our thoughts turned to the tamahagane

smelting process. The phosphide eutectic mechanism as we know does not fit the Japanese reality. The chemical composition of ore and purity of steel produced in the Japanese process exclude the phosphorus as a causative factor of high carburization (Suzuki and Nagata 1999; Inoue 2002, p.196). The only known mechanism able to do this was carburization by 'remelting'. The next three experiments were focused on receiving this process directly in the bloomery furnace. The results of two of them are be presented below.

Experiment 1

Experiment one, carried out on 15th June 2012, was conducted in thin-walled, free-standing shaft furnace on an oval plan, modelled on the ancient furnace from Loděnice, dated on third to fourth centuries AD (Pleiner 2000, p.175). It was built of clay mixed with straw and gravel on thin clay film (≈ 1 cm) isolating it from the substrate. The internal diameter of furnace was 30 x 32 cm on the bottom and narrowed to 24 cm at the top of the shaft. The wall thickness was about 6-7 cm in lower parts. The ore used in the process was a poor-quality and high silica content 'ferruginous-sand' gathered from the fields beneath the Starachowice. It was double roasted on wooden piles with the total time estimated at about ten hours. A drain hole the size of 7x7 cm was placed on the base of the furnace. The blowing hole had an internal diameter of 35 mm and was located 20 cm above the furnace bottom with the inclination angle of some 15 degrees (see Figure 8). It was powered by the two alternately blowing, large hand-bellows, each of about 70-80 l capacity, which made it possible to maintain a continuous draft for almost the entire duration of process (with a few breaks in order to make necessary repairs to the shaft). Bellows nozzles were combined into one by a wooden tee. The tip of the tuyère was not connected with the furnace and was distanced at about 2-3 cm from the wall. The charcoal used was commercially made beech, and was crushed and selected to a size range of 30-50 mm.

Some 20 kg of roasted ore and 45 kg of charcoal (including preheating) was used in a total time of 4.5 hours. Before the first ore loading, the furnace was preheated for about one hour. In the next three hours of proper smelting, ore and charcoal were added alternately in 1:1 ratio in the quantity of 2.5 kg each. After the last ore charge the furnace was filled only with charcoal and worked for the next half hour. Slag was tapped out every 30 minutes. After this time the furnace was disassembled, and it showed the unusual bloom's location. It was attached to the furnace's side wall at an angle of 90 degrees, relative to the tuyère (see Figure 10, left). The slag, containing a small lumps of iron, covered the furnace bottom. When attempting to compact the bloom, it disintegrated into several pieces. The total result of the process was 2.2 kg of steel, mostly highly carburized.

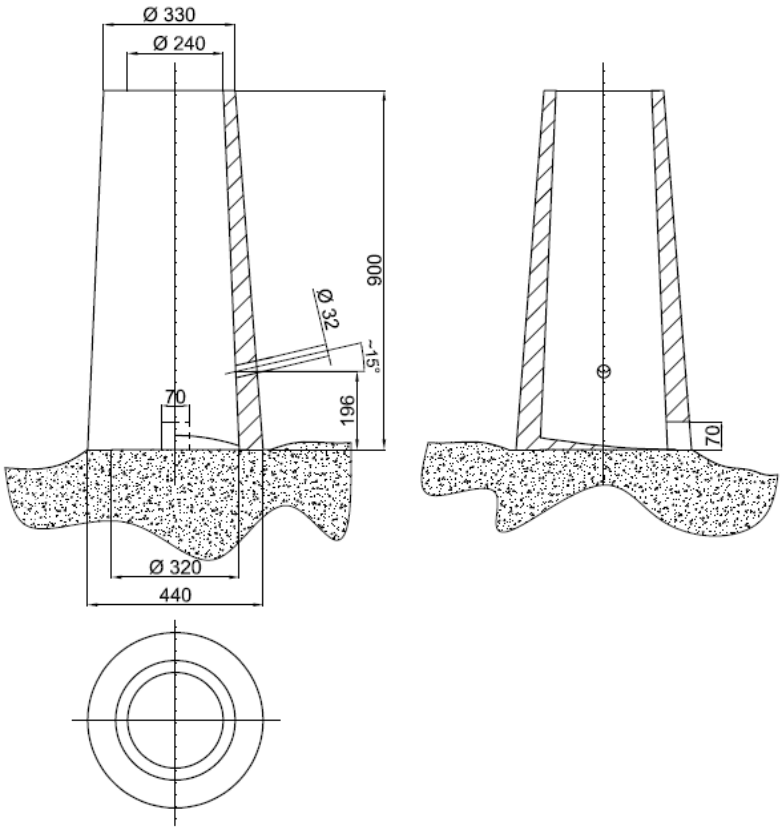

Fig 8. Cross-section and plan of the furnace from Experiment 1.

Experiment 2

This experiment from beginning did not go as planned. After just a little over two hours of operation the smelt was stopped by rain in the middle of the process. However, the results appeared to be quite interesting and worth for examining. The experiment was conducted on 12 September 2012, in a Japanese modelled furnace that imitated a modern furnace used by the Japanese swordsmiths (see Figure 9). The smelting process was preceded by two days of preparation. The construction of the furnace was the first step. It was built on a square plan using an ordinary bricks, but with thick (1-2 cm) internal clay lining. The size of the chamber was 26 x 26 cm in the lower part with a 10-11 cm thick wall and narrowed to 22 cm at the mouth of the shaft with walls 6-7 cm thick. The total height of construction was 110 cm, including a 10 cm base. The bottom of the furnace was shaped to a gutter form of v-shaped cross-section for better slag removal. The drain hole (80x80 mm) was situated on the sidewall of furnace. The air was supplied by an electric blower through a 35 mm tuyère embedded into the wall, in quantity between 120-200 l/min and adjusted to the current needs. From time to time the blast was being increased for a few minutes to about 300 l/min. The tuyère was located 20 cm above the furnace bottom with inclination angle of some 20 degrees.

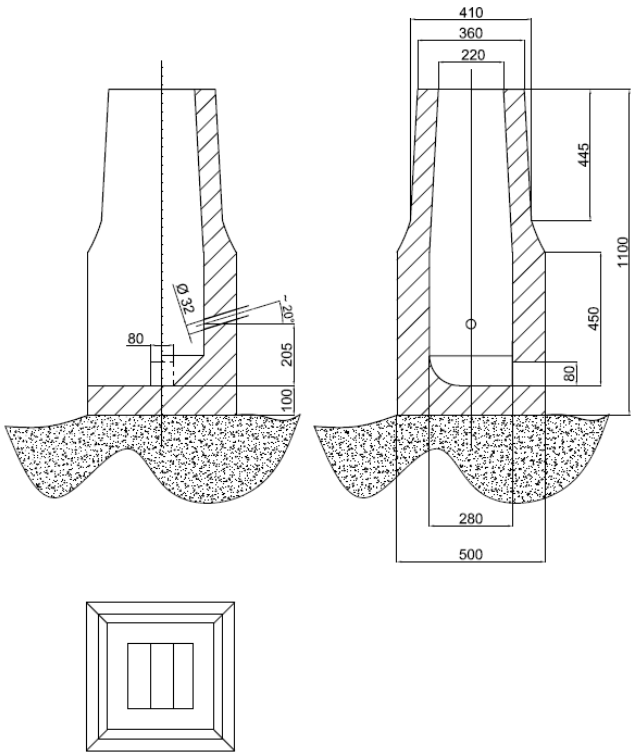

Fig 9. Cross section and plan of the furnace from Experiment 2.

The ore used in the process consisted of two types of limonite. First one was the same 'ferruginous-sands' as in Experiment 1. The second type was limonite imported from Bosnia and Herzegovina, used as a supplement to a proper batch by the Ironworks in Katowice. The composition of this ore was shown in Table 1. The ore was roasted twice on an iron grill fuelled by pine and oak wood in the total time of eight hours. It was also crushed to the fraction of less than 1.5 cm. Once again, the charcoal used was a commercially made of beech, crushed and selected to a size range of 30-70 mm.

Ore components	H_2O	Fe	Mn	CaO	MgO	Al_2O_3	P_2O_5	S	C	Na_2O	K_2O	Zn
Percentage content (%)	12,20	54,69	1,64	0,24	0,56	0,63	0,11	0,012	0,89	0,03	0,07	0,01

Table 1. The composition of Bosnian ore used in Experiment 2. The data are given for selected elements only.

The smelt was started at 12:30 pm. The furnace was dried the day before. For 1.5 hours it was heated only by wood. After this time it was filled with a large size of charcoal and warmed up to the appropriate temperature. In the same time the blast began. The first charge of ore in the amount of 4 kg was at 2:40 pm, more than two hours after ignition. Next charges for 3 kg each were held approximately every 25 minutes. The ore portions were separated by charcoal in amounts of 3 kg,

except for the 3rd charge, after which double charcoal was added. Slag was tapped out every 20-30 minutes, and most of it was strongly fluidized. About 5 pm, as was mentioned before, the process had to be terminated because of a sudden deterioration of the weather.

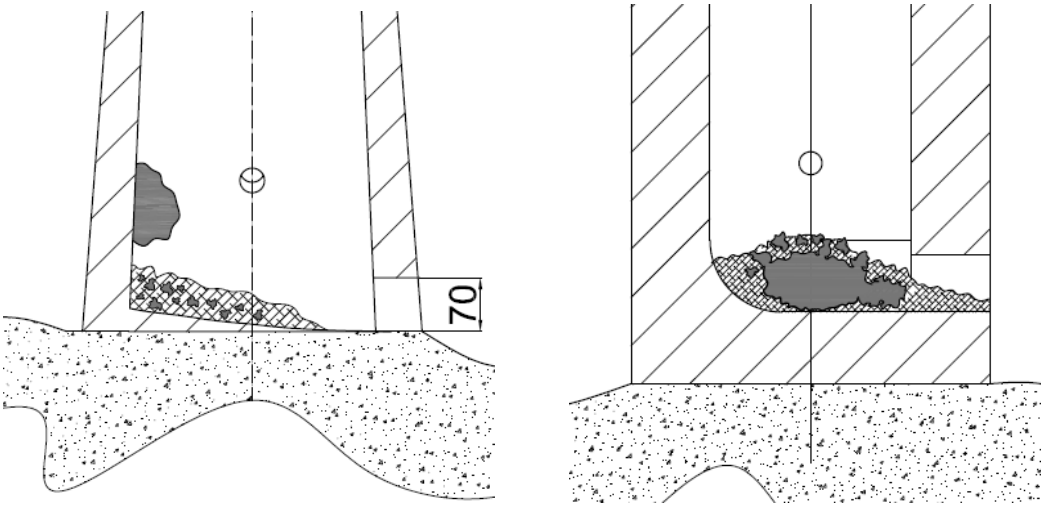

Fig 10. The locations of blooms from Experiment 1 (left) and Experiment 2 (right).

The entire process consumed about 30 kg of charcoal, 19 kg of ore and a wheelbarrow of wood. However, these latter two portions of ore did not manage to get down to the level of blast, so basically I had to accept that only about 13 kg of ore was used in the smelt. The raw bloom weighed 3.8 kg, but the process has not been brought to the end and contained a lot of slag. It was situated in the gutter at the bottom of the furnace in the normal position of bloom (see Figure 10, right). After separation of the impurities 1.7 kg of iron was left. Most of the bloom was dense and uniform but in in the upper and front surface there were visible parts that were not fully integrated with main mass. They had been disconnected during slag separations.

Examination results of iron from experiment 1

Because the bloom from the experiment 1 was crushed, two parts have been chosen for examination (see Figure 11). The samples of them were taken, polished and photographed after etching with 3% nital. Both of the samples had a fairly porous structure with numerous slag inclusions, charcoal fragments and voids.

Sample No.1.1 has a mostly homogeneous structure of pearlite with numerous oxide inclusions and many areas of transformed ledeburite (see Figure 14). Very few areas showed the local occurrence of ferrite-pearlitic structures usually associated with the fusion spots—perhaps caused by the presence of phosphide eutectic (see Figure 15). The fusion spots occur also in pearlitic areas (see Figures 16,18 and 19). They attracting carbon from adjacent spaces and creating a characteristic band on the grain boundaries. Besides, numerous fusions with ledeburite structure were observed on the whole cross-section of sample (see Figure 17).

Sample No.1.2 has a more heterogeneous structure. The dominating phase is pearlite, but in some parts a ferrite network can be observed on the pearlitic background (see Figure 20). Ferritic educts in Widmanstätten orientation are mostly located on the edges of the sample (see Figure 21). Moreover, similarly as in the sample No.1.1 we can observe plenty of fusion spots with phosphide eutectic or ledeburite content (see Figure 22-24). A primary segregation of elements can be also observed in some ferrite educts (see Figure 23,25).

The presented structures are not easy to interpret. A homogeneous pearlitic structure occurring in almost the entire volume of selected lumps may suggest a diffusional carburization of reduced iron parts to the eutectoid point, before their unification. In an appropriately high temperature, caused by fuel combustion or rapid oxidation of iron surface, which is a strongly exothermic reaction and could easily raise the temperature, the solidus line of 0,77% composition has been exceeded and the alloy has melted. These areas absorbed carbon to the eutectic level and created ledeburite and ferrite hoops on the grain boundaries that were areas of fusion. However, it is hard to explain why the carbon from the eutectic structures did not diffuse to the surrounding areas and did not create any hypereutectoid structures after staying few hours at such a high temperature. A ferrite-pearlitic structure on the edge of sample No.1.2 may be caused by superficial decarburization of lump. Unfortunately, the expected hypoeutectic structures around the ledeburite areas, which may indicate them as a carburization sources, have not been observed but it does not exclude the existence of this mechanism. There is a need for further studies on large numbers of samples from various stages of smelting process.

Examination results of iron from experiment 2

Detailed examination of experiment 2 samples have revealed a grey cast iron structure on all the parts of 'bloom'. With regard to the assumptions of the experiment, this smelt is a failure. However, considering the conditions in which the process was held, its results can bring a lot of information about the reactions that occur inside the furnace during the smelting operation.

In contrast to the bloom from experiment 1, the iron obtained in this process was a dense and homogeneous lump with only a few fragments not integrated with the whole mass. The voids occurring on the cross-section derived most likely from fragments of burnt charcoal or gas bubbles trapped in the mass of iron. Three samples were taken to analyse. Two of them from the main iron mass (see Figure 11) and the third one from one of the non-integrated parts (see Figure 12).

Sample No.2.1 was taken from the lower part of 'bloom'. It consisted of a homogeneous structure of pearlitic grey cast iron with only minor ferritic educts, mostly on the grain boundaries (see Figure 26). In some areas the needle-shaped ferrite can be also observed (see Figure 27). The graphite flakes are long, relatively thin and slightly curved in some areas. They demonstrate an uneven distribution in metal. The second sample taken from the top of the 'bloom' and labelled as No.2.2, has a similar structure, but with this difference that there are very large numbers of phosphide eutectic, which occurred in the whole element (see Figures 28-29). The last sample (No.2.3) is characterized by pearlite-ferritic matrix and multitude of phosphide eutectic, similar to sample No.2.2. Also the needle-shaped ferrite also occurs much more frequently than previously (see Figures 30-31).

The structures presented above are the result of melting and slow cooling of an alloy in the carburizing atmosphere with a large content of carbon monoxide. It is interesting that, despite such a low air rate, it was possible to create the above structure. Possibly the small size of the furnace chamber, thick walls and low but constant air flow, which does not cool the charge, created appropriate conditions for the appearance of the liquid phase. Perhaps the phosphide eutectic, which has low melting point, also contributed to this. Usually the production of grey cast iron is caused by slow cooling, allowing the formation of the graphite flakes. However, due to the course of the process described above, it is clear that it cannot explain the occurrence of this phenomenon. It seems that the cause of graphitization here may be the silica- and phosphorus-rich ore composition. Both elements are known as graphitizing factors, favouring the formation of grey cast iron (Crew, et al. 2011, p.251). The high phosphorus content is confirmed by multitudes of phosphide eutectic occurring virtually on the entire volume of metal.

C	S	Mn	P	Si
3,65 %	0,020%	0,10%	0,164%	0,13%

Table 2. The analyses of cast iron from Exp.2.

Discussion

The experiments gave a detailed view of the entire spectrum of processes taking place in a bloomery furnace. It includes diffusion carburizing, autonomous melting after crossing the solidus point, partial fusion of iron surface and fusion connected with phosphide eutectic. It also shows that any structure from the iron-carbon system can be easily achievable in the bloomery process and controlled by a skilled smelter. Of course, the conducted examination does not explain the complexity of carburizing mechanisms, but it clearly shows a wide range of possibilities, none of which should be marginalized. To resolve any suppositions and doubts arising in connection with the conducted experiments further detailed studies are required. The problem has not been widely discussed so far in the literature.

It was not possible to definitely prove that the main factor of high carburization obtained in smelting processes was carburization by 'remelting'. However, the examination results do not exclude this possibility. Staying for an extended time at such a high temperature could cause a wide diffusion of carbon that did not leave more significant traces. The transitions between eutectoid and hypoeutectoid structure observed in sample No.1.2 and identified as a superficial decarburization could be a border point of internal carbon diffusion as well. However, we need a further studies and examinations on this issue.

I do not see any contraindications to the presence of this process in a bloomery furnace. The rapid oxidation of iron definitely occurs during the smelting operation and may be watched in form of bright sparks outgoing very often from the blowing or drain holes. A sudden rise of temperature accompanying this phenomenon should have some influence on the surrounding iron parts that left

in a metallic state and created the bloom. The only question, which we are obliged to answer on this stage of our analysis, is the extent of this influence and whether they are large enough to affect the final result of smelting process. Accordingly, further experiments are going to be carried out this year to resolve the remaining doubts.

Acknowledgments

These experiments were part of research project No 611 076 (84/R) *Identification of metallurgical residues of bloomery iron processing*, implemented as a part of author's PhD studies at The Institute of History, The Jan Kochanowski University in Kielce.

Metallographic and chemical analyses were conducted on Faculty of Metal Engineering and Industrial Computer Science, AGH University of Science and Technology in Kraków. Special thanks to Dr Eng. Ireneusz Suliga for help in analyses and interpretation of micro-structures, MA Marta Góra for chemical analyzes, Prof. Stanisław Dymek for access to the laboratory, Prof. Tomasz Polański for language correction of this paper and Dr Szymon Orzechowski for the supervision of my research.

Drawings of furnaces schemes was made by Eng. Przemysław Wrona.

Reference list

Biringuccio V., 1540. *De la Pirotechnia libri X*, Translated from Italian by C. S. Smith and M. T. Gnudi., 1966. London.

Crew, P., 2004. Cast Iron from a Bloomery Furnace, *Historical Metallurgy Society News,* No. 57, pp.1-2.

Crew, P., Charlton, M., Dillmann, P., Fluzin, P., Salter, C., and Truffaut, E., 2011. Cast iron from a bloomery furnace. In J. Hošek, H. Cleere and L. Mihok, ed. *The archaeometallurgy of iron. Recent developments in archaeological and Scientific Research*, Praha, pp.239-262.

Evenstad, O., 1968. A treatise on Iron Ore as Found In the Bogs and Swamps of Norway and the Process of Turning it into Iron and steel. Abridged translation of Evenstad 1790 by Niels L. Jensen, *Bulletin of the Historical Metallurgy Group*, vol. 2, issue 2, pp.61-65.

Forbes, R. J., 1950. *Metallurgy in Antiquity*, Leiden.

Inoue*, T.,* 1997. The Japanese Sword. The Material, Manufacturing and Computer Simulation of Quenching Process*, Materials Science Research International*, vol. 3, issue 4, pp. 193-203.

Kapp, L., Kapp, H., Yoshihara, Y., 1987. *The craft of the Japanese sword*, Kodansha International.

Kędzierski, Z., Stępiński, J., 2006. Metaloznawstwo żelaza z okresu rzymskiego na ziemiach polskich, In Sz. Orzechowski and I. Suliga, ed. *50 lat badań nad starożytnym hutnictwem świętokrzyskim. Archeologia – Metalurgia - Edukacja*, Kielce, pp.177-192.

Knau, H. L., Beier, T., and Sönnecken, M., 2001. Iron Works and Water Power - the Development of Mechanical Hammer Works in the "Südgebirge", *Acta Metallurgica Slovaca*, vol. 7, pp.127-143.

Krawczuk, A., Piaskowski, J., 1958. Metalurgia w pismach Arystotelesa, *Kwartalnik Historii Kultury Materialnej*, vol. 6, issue 3, pp.334-335.

Lucas, A. R., 2005. Industrial milling in the ancient and Medieval Worlds, *Technology and Culture*, vol. 46, issue 1, pp.1-30.

Nosek, E., 1966. Niektóre zabytki żelazne z terenu Gór Świętokrzyskich w świetle badań metaloznawczych, *Materiały Archeologiczne*, vol. 7, pp.179-184.

Piaskowski, J., 1960. Metaloznawcze badania wyrobów żelaznych z okresu halsztackiego i lateńskiego pochodzących z Małopolski*, Materiały Archeologiczne*, vol. 2, pp.201-220.

Pleiner, R., 2000. *Iron in Archaeology. The European Bloomery Smelters*, Praha.

Pleiner, R., 2006. *Iron in Archaeology. Early European Blacksmiths*, Praha.

Porta a Neopolitane, John Baptist, 1638. *Natural Magic in XX books*, London.

Radwan, M., 1963. *Rudy, kuźnice i huty żelaza w Polsce*, Warszawa.

Rehder, J. E., 1989. Ancient carburization of iron to steel, *Archeomaterials*, vol. 3, pp.27-37.

Sauder, L., 2010. *Making Steel in the "Aristotle Furnace"*, [pdf] Available at: <http://www.leesauder.com/pdfs/Aristotle's%20Steel.pdf> [Accessed 03 August 2012].

Suzuki, T., Nagata, K., 1999. Effect of the Charge of "Komori" Iron Sand on the Properties of "Tamahagane" Steel Produced by "Tatara" Operation, *Tetsu to Hagane*, vol. 85, issue 12, pp. 911-916.

Theophilus Presbyter, 1998. *Diversarum Artium Schedula. Średniowieczny zbiór przepisów o sztukach rozmaitych,* Translated from Latin by S. Kobielus., Kraków.

Wagner, D., 1990. Ancient carburization of iron to steel: a comment*, Archeomaterials*, vol. 4, pp.111-117.

Wrona, A., 2012. Carburizing by "re-melting". The new perspective on the problem of thermo-chemical treatment of iron in antiquity [in polish], In J. Gancarski, ed. *Skanseny archeologiczne i archeologia eksperymentalna,* Krosno, pp. 611-630.

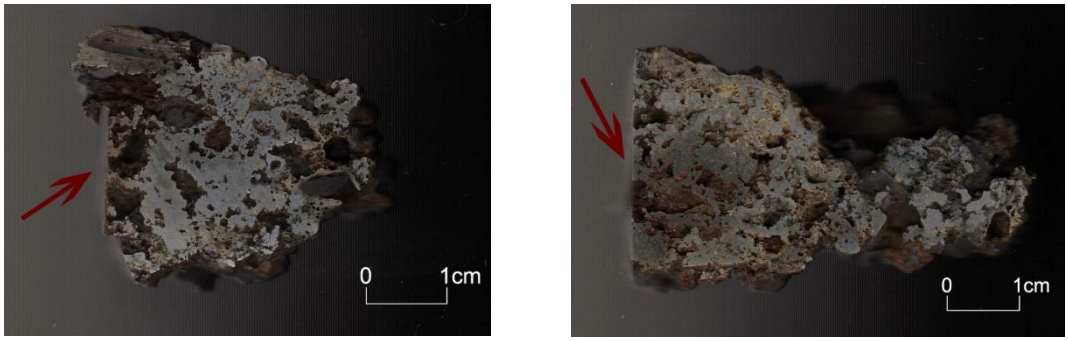

Fig.11 Iron lumps from Exp.1. Red arrows indicate the location of taken samples: No.1.1 (left), No.1.2 (right).

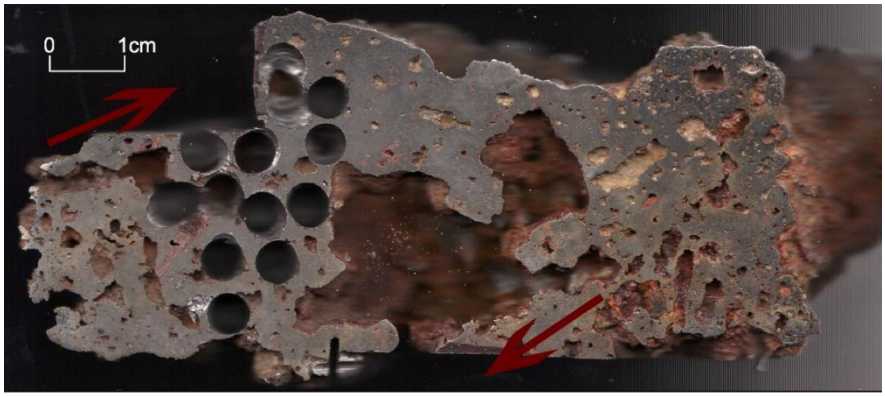

Fig.12 Iron "bloom" from Exp.2. Red arrows indicate the location of taken samples: No.2.1 (up), No.2.2 (down).

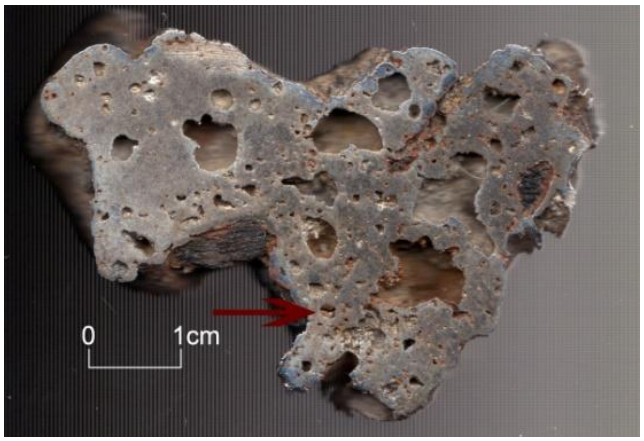

Fig. 13 Iron lump from Exp.2. Red arrows indicate the location of taken sample No.2.3.

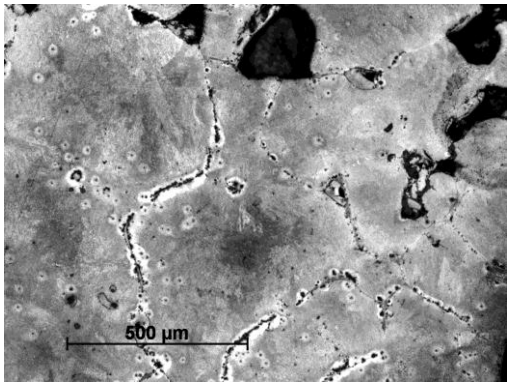

Fig.14 Micro-photograph of sample No.1.1. Typical structure of sample. Coarse-grained pearlite with fusion spots on the grain boundaries.

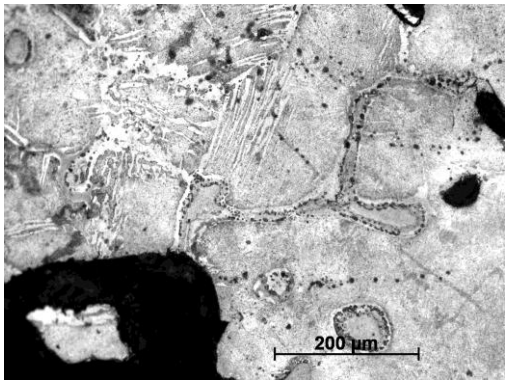

Fig.15 Micro-photograph of sample No.1.1. Ferrite-pearlitic area with extensive fusion areas - probably phosphide eutectic.

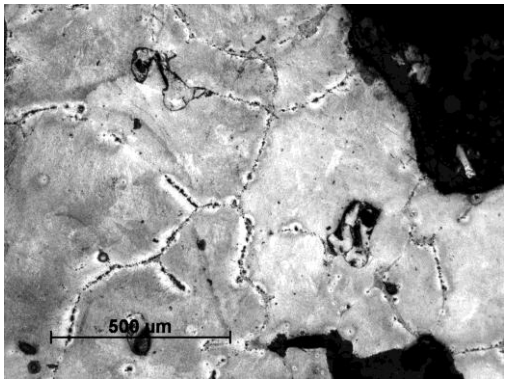

Fig.16 Micro-photograph of sample No.1.1. Fusion spots on pearlite grain boundaries.

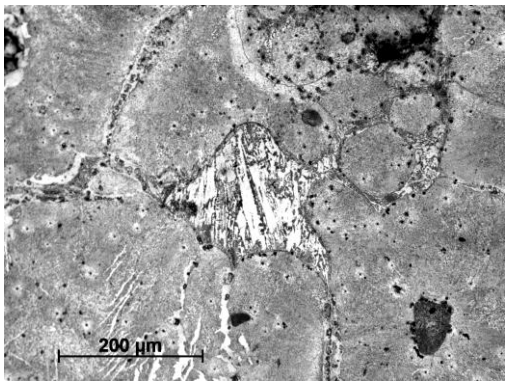

Fig.17 Micro-photograph of sample No.1.1. Characteristic for sample fusions with ledeburite structure.

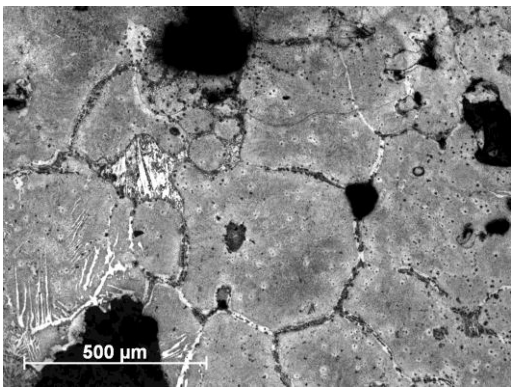

Fig.18 Micro-photograph of sample No.1.1. Wide variety of structures occurring in the sample: pearlite, rare ferrite and numerous fusion spots.

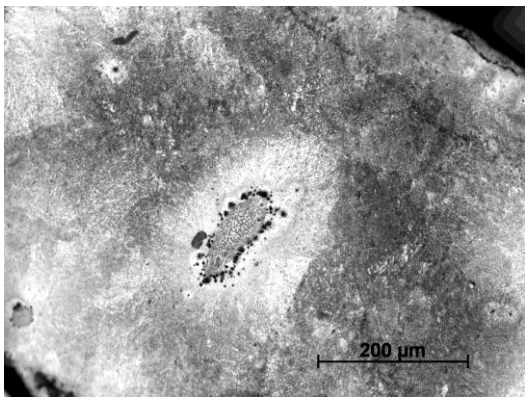

Fig.19 Micro-photograph of sample No.1.1. Phosphide eutectic on the pearlitic background.

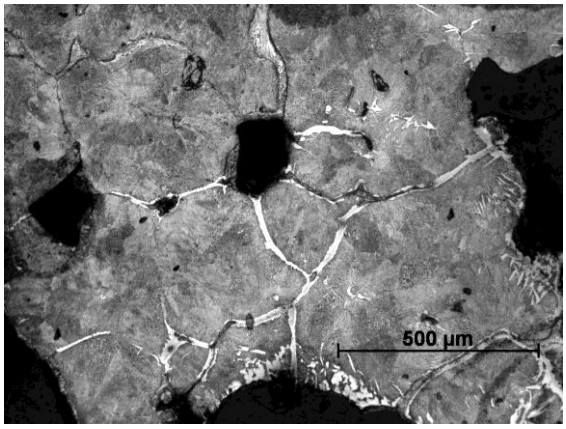

Fig.20 Micro-photograph of sample No.1.2. Typical structure of sample: pearlite, ferrite and various fusion spots.

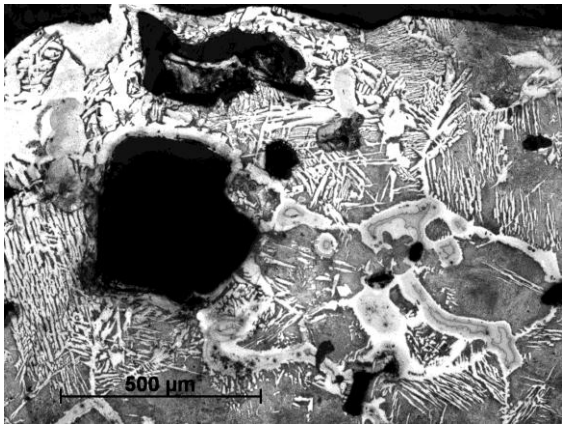

Fig.21 Micro-photograph of sample No.1.2. Ferrite network on the pearlitic background. Locally, ferrite in Widmanstätten orientation.

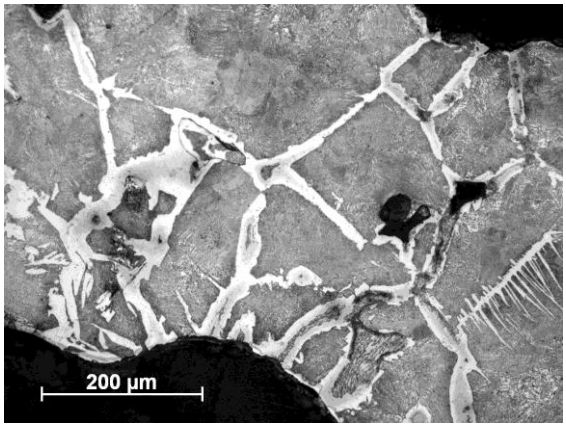

Fig.22 Micro-photograph of sample No.1.2. Pearlite with various fusion spots on the grain boundaries.

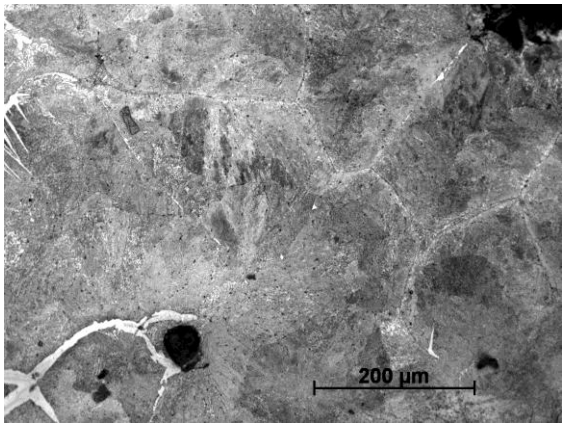

Fig.23 Micro-photograph of sample No.1.2. Pearlite-ferritic structure with phosphide eutectic. Ferrite with primal segregation of elements.

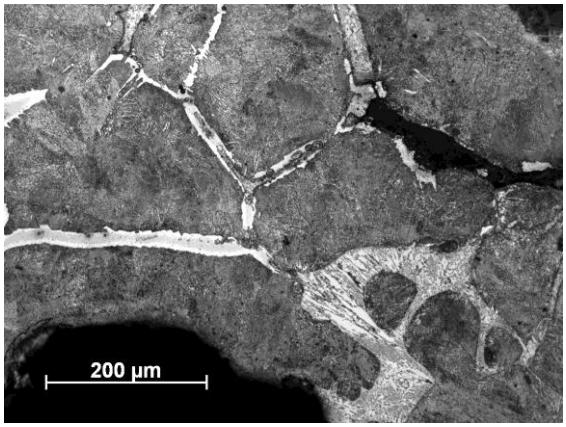

Fig.24 Micro-photograph of sample No.1.2. Fusions on the pearlite boundaries.

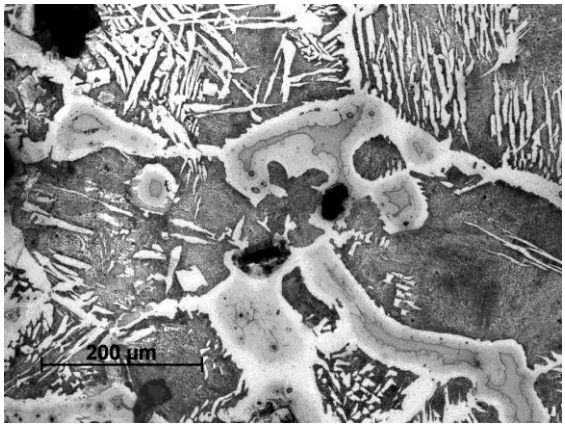

Fig.25 Micro-photograph of sample No.1.2. Ferrite with primal segregation of elements.

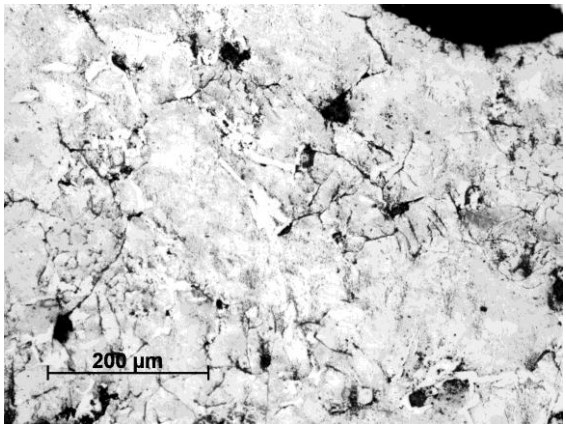

Fig.26 Micro-photograph of sample No.2.1. The structure of pearlitic grey cast iron. Graphite flakes in diverse clusters. White spots - ferrite (not etched).

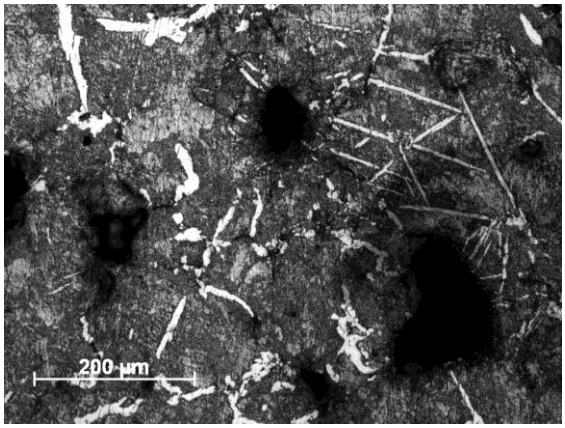

Fig.27 Micro-photograph of sample No.2.1. Pearlite-ferritic matrix of grey cast iron. Locally a needle-shaped ferrite.

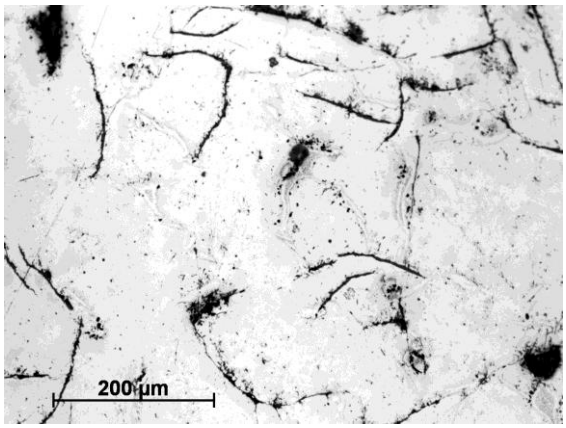

Fig.28 Micro-photograph of sample No.2.2. Graphite flakes and phosphide eutectic spots on pearlite-feritic matrix (not etched).

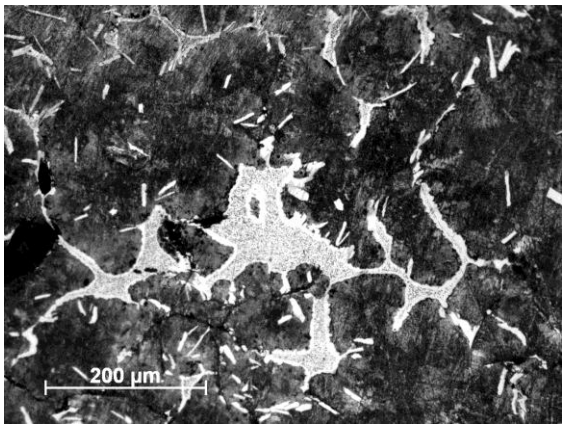

Fig.29 Micro-photograph of sample No.2.2. Phosphide eutectics on the pearlite-ferritic matrix.

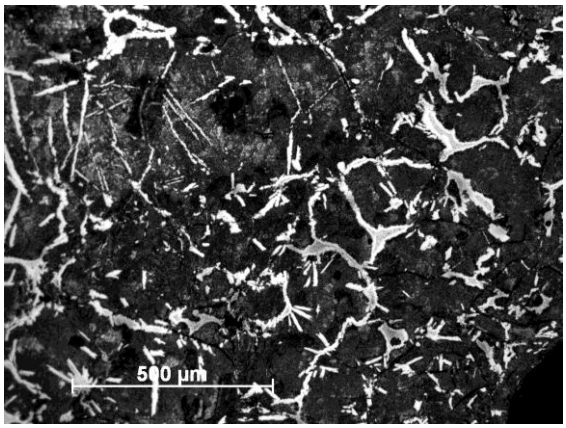

Fig.30 Micro-photograph of sample No.2.3. Typical structure of sample. Pearlite, ferrite and phosphide eutectic.

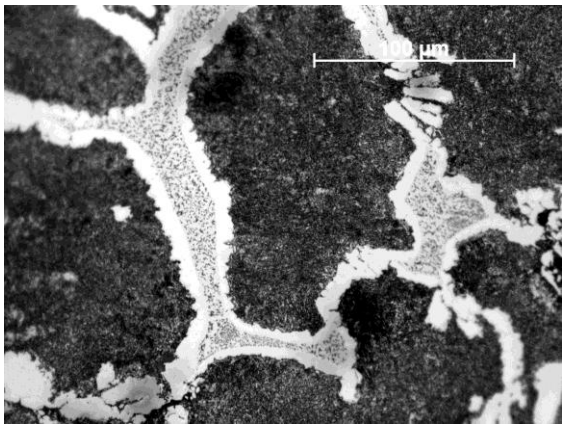

Fig.31 Micro-photograph of sample No.2.3. Phosphide eutectic.